J|A|C|S
ARTICLES
Published on Web 06/22/2002

Chemical Bonding in Biguanidinium Dinitramide and Biguanidinium Bis-Dinitramide from Experimental X-ray Diffraction Data

Elizabeth A. Zhurova, Anthony Martin, and A. Alan Pinkerton*

Contribution from the Department of Chemistry, University of Toledo, 2801 West Bancroft Street, Toledo, Ohio 43606

Received November 27, 2001

Abstract: The electron density and related properties of biguanidinium dinitramide (BIGH)(DN) and biguanidinium bis-dinitramide $(BIGH_2)(DN)_2$ crystals (space groups $P\bar{1}$ and $C2/c$) have been determined from low-temperature (90(1) K) X-ray diffraction experiments. The Hansen−Coppens multipole model as implemented in the XD program gave $R = 0.0247$ and 0.0201 (all reflections) which allowed the calculation of the electron density and Laplacian distributions. The bonding (3,−1) critical points were also found. The analysis of the results shows that Bader's topological theory provides a more useful description of the chemical bonding in the studied crystals as compared to the classical analysis of deformation densities. The hydrogen bonding in the crystals was analyzed. The atomic charges were integrated over the atomic basins.

Introduction

In recent years, there has been a great interest in the development of new solid energetic materials, especially propellants with low signatures. Desired properties for this class of compounds are halogen-free, nitrogen- and oxygen-rich molecular composition, high densities, and a high heat of formation.[1] The ability of the dinitramide (DN) anion to form stable oxygen-rich salts with high densities with a variety of cations makes it a promising candidate in the development of energetic oxidizers.[2] The high density[3,4] of biguanidinium dinitramide (BIGH)(DN) and biguanidinium bis-dinitramide $(BIGH_2)(DN)_2$ crystals, partially because of the molecular shape similarity between anion and cations, makes these crystals very interesting candidates for a more detailed study.

The crystal structures of biguanidinium dinitramide (BIGH)(DN) and biguanidinium bis-dinitramide $(BIGH_2)(DN)_2$ have been reported previously[3] and consist of isolated cations and anions linked by extensive hydrogen bonding.

Both monoprotonated $(BIGH)^+$ and diprotonated $(BIGH_2)^{2+}$ biguanidinium cations are composed of two planar halves with one nitrogen atom in common. The two halves are twisted with respect to each other with twist angles (see below) of 42.1° (BIGH) and 43.8° ($BIGH_2$). All bonds are relatively short because of extensive π-delocalization.[5] The protonation of the bridge N atom leads to a small increase in the C−N bridge bond lengths (as compared to the monoprotonated cation) with a concomitant shortening of the terminal C−N bonds.[6] It was reported[7] that the energy of protonation of neutral biguanide was unusually high ($\Delta H = -95$ kJ/mol) and the addition of a second proton was also rather energetic ($\Delta H = -21$ kJ/mol). The high enthalpy of protonation was interpreted as being because of the replacement of two localized double bonds by the formation of a cation whose π electrons were delocalized over the whole molecule.

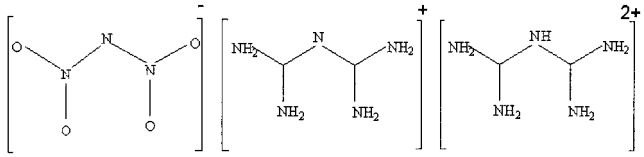

The (DN) anion has a surprisingly variable and asymmetric structure in different compounds.[1] The twist angles used to describe the mutual arrangement of the two nitro groups can be calculated from the two torsion angles of the NO_2 groups out of the NNN plane and then by averaging these two values.[8] These twist angles are 7.1 and 28.8° for the (BIGH)(DN) and $(BIGH_2)(DN)_2$ crystals, correspondingly. The difference of the

* To whom correspondence should be addressed. E-mail: apinker@uoft02.utoledo.edu.

(1) Tanbug, R.; Kirschbaum, K.; Pinkerton, A. A. *J. Chem. Crystallogr.* **1999**, *29*, 45−55.
(2) Christe, K. O.; Wilson, W. W.; Petrie, M. A.; Michels, H. H.; Bottaro, J. C.; Gilardi, R. *Inorg. Chem.* **1996**, *35*, 5068−5071.
(3) Martin, A.; Pinkerton, A. A.; Gilardi, R. D.; Bottaro, J. C. *Acta Crystallogr.* **1997**, *B53*, 504−512.
(4) Gilardi, R. D.; Karle, J. In *Chemistry of Energetic Materials*; Olah, G. A., Squire, D. R., Eds.; Academic Press: San Diego, 1991; pp 1−26.
(5) Pinkerton, A. A.; Schwarzenbach, D. *J. Chem. Soc., Dalton Trans.* **1978**, 989−996.
(6) Martin, A.; Pinkerton, A. A.; Schiemann, A. *Acta Crystallogr.* **1996**, *C52*, 966−970. Martin, A.; Pinkerton, A. A. *Acta Crystallogr.* **1996**, *C52*, 1048−1052.
(7) Fabrizzi, L.; Micheloni, M.; Paoletti, P.; Schwarzenbach, D. *J. Am. Chem. Soc.* **1977**, *99*, 5574−5576.
(8) Shlyapochnikov, V. A.; Tafipolsky, M. A.; Tokmakov, I. V.; Baskir, E. S.; Anikin, O. V.; Strelenko, Yu. A.; Lukyanov, O. A.; Tartakovsky, V. A. *J. Mol. Struct.* **2001**, *559*, 147−166.

anion N−N bond lengths is 0.023 Å for (BIGH)(DN) and 0.037 Å for $(BIGH_2)(DN)_2$. These bond lengths of 1.35−1.39 Å are not as short as N−N double bonds (1.245 Å) and not as long as N−N single bonds (1.454 Å). The N(2)−N(1)−N(3) and all of the N(1)−N(2),(3)−O angles of 111.2−126.8° show that the geometry at nitrogen is of an intermediate type, between the ideal sp^2 and sp^3. It has been pointed out[9] that if the central nitrogen is sp^3 hybridized, then a 27° rotation of the nitro groups from the central NNN plane makes them approximately perpendicular to the lone pair orbitals, thereby optimizing possible conjugation. On the other hand, if the central nitrogen is sp^2 hybridized, then one lone pair will be in the p orbital perpendicular to the NNN plane in which case a 0° twist would optimize possible conjugation for the nitro groups. From a steric point of view, a twist of 0° or 90° would maximize or minimize steric repulsions between the closest nitro oxygen atoms.[10] Several theoretical calculations[2,11] showed that the potential energy surface for rotation of the nitro groups is very shallow. This explains the variety of twist angles observed in the series of dinitramide salts.[1] Obviously, the metrical parameters of the (DN) anion are strongly influenced by the environment.

The traditional way to study chemical bonding in crystals and molecules experimentally is to analyze the deformation electron density $\delta\rho(\mathbf{r})$ distribution.[12] This function was introduced in 1956 by Roux et al.[13] and has been widely used since then. It represents the difference between the electron density (ED) of the system $\rho(\mathbf{r})$ and the ED of a set of spherically averaged noninteracting neutral atoms $\rho'(\mathbf{r})$, placed at the same positions as the atoms of the system. Therefore, it describes the redistribution of electrons after neutral atoms combine to form the crystal (or molecule). One can thus expect maxima associated with the positions of chemical bonds, lone pairs, etc.

Another approach, which has gained popularity in the past decade, is the analysis of the total electron density using the theory of atoms in molecules (AIM).[14] This theory is rooted in quantum mechanics;[15] it describes a crystal in terms of the ED, $\rho(\mathbf{r})$, its gradient vector field, $\nabla\rho(\mathbf{r})$, ED curvature, critical point ($\nabla\rho(\mathbf{r}_c) = 0$) positions, and their characteristics.[16] The critical point (CP) is defined by rank, the number of nonzero eigenvalues of the diagonalized Hessian matrix λ_i, and signature, the sum of the algebraic signs of λ_i. The ED exhibits four kinds of nondegenerate CPs of rank 3, with a (3,−1) saddle point corresponding to a chemical bond in the crystal or molecule. In the $\nabla\rho(\mathbf{r})$ field, pairs of gradient lines originating at a (3,−1) CP and terminating at two neighboring nuclei (determined by the eigenvector corresponding to the only positive eigenvalue of the Hessian, λ_3, at the CP) form the atomic interaction lines along which the ED decreases for any lateral displacement. At equilibrium, this line is named a bond path containing the associated (3,−1) bond CP. The negative eigenvalues λ_1 and λ_2 at the bond CP correspond to the directions normal to the bond path and measure the degree of ED contraction toward this point; $\lambda_3 > 0$ measures the degree of ED contraction toward each of the neighboring nuclei. The spatial distribution of the Laplacian of the ED, $\nabla^2\rho(\mathbf{r})$, characterizes regions of concentration and depletion of electrons. In the view of the local virial theorem,[14] $\nabla^2\rho(\mathbf{r})$ can be interpreted as the local balance between the kinetic and potential energy of a molecule. The sign of the Laplacian at the bond (3,−1) CP, obtained from summing the principal curvatures of the ED at the CP, reflects the character of the atomic interactions. If the electrons are locally concentrated in the bond CP ($\nabla^2\rho(\mathbf{r}_c) < 0$), then ED is shared by both nuclei, typical for covalent bonds. If electrons are concentrated in each of the atomic basins separately ($\nabla^2\rho(\mathbf{r}_c) > 0$), the interaction type is closed-shell, typical for ionic and hydrogen bonds, as well as van der Waals interactions.[17−18] The nuclei of neighboring atoms in a crystal are separated in the $\nabla\rho(\mathbf{r})$ field by surfaces of zero flux defined by the gradient lines terminating at the (3,−1) CPs. These surfaces define the bounded atoms in terms of the ED. The properties of these bounded atoms are defined by the quantum action principle;[12,19] they are characteristic and additive.[20]

Experimental and Refinements

Crystals of biguanidinium dinitramide (BIGH)(DN) and biguanidinium bis-dinitramide $(BIGH_2)(DN)_2$ were grown from dry acetonitrile by slow evaporation. Colorless parallelepiped crystals with well-defined faces were selected. Preliminary examinations and data collections were performed with Mo Kα radiation on an Enraf-Nonius CAD4 kappa axis diffractometer using an Oxford Cryostream cooling device. Cell constants and orientation matrices were obtained from least-squares refinement, using the setting angles of 25 reflections (Table 1), measured by the diagonal slit method of centering. The intensity data were collected using the $\omega - 2\theta$ scan technique, the scan rate being varied from 0.5 to 7.0 °/min. A full reciprocal sphere of data up to $\sin\theta/\lambda = 0.7$ Å^{-1} and half a sphere for $0.7 < \sin\theta/\lambda < 1.34$ Å^{-1} were collected (Table 1). For the high-angle data, only reflections calculated[21] to be above $3\sigma(I)$ were measured. The stability of the measurement was checked by the measuring of three representative orthogonal reflections every 50 min. Data reduction[22] was carried out as follows. The peak profiles were analyzed and Lorentz and polarization corrections applied to the data using the programs REFPK and BGLP. A linear scaling correction was applied using the computer program SCALE3. An analytical absorption correction was applied using the program ABSORB.[23] A correction for errors in the measured crystal shape, absorption due to the capillary and glue, and X-ray beam inhomogeneity was applied in the program SORTAV. An empirical TDS correction was applied using the computer program TDSCORR. The maximum correction applied was 27.1% for the (BIGH)(DN) crystal.

The crystal structures were resolved and preliminary refinements carried out with the SHELXTL program suite.[24] The Hansen−Coppens[25]

(9) Politzer, P.; Seminario, J. M.; Concha, M. C.; Redfern, P. C. *J. Mol. Struct. THEOCHEM* **1993**, *287*, 235−240.
(10) Butcher, R. J.; Gilardi, R. D. *J. Chem. Crystallogr.* **1998**, *28*, 95−104.
(11) Politzer, P.; Seminario, J. M. *Chem. Phys. Lett.* **1993**, *216*, 348−352. Michels, H. H.; Montgomery, J. A., Jr. *J. Phys. Chem.* **1993**, *97*, 6602−6606. Mebel, A. M.; Lin, M. C.; Morokuma, K.; Melius, C. F. *J. Phys. Chem.* **1995**, *99*, 6842−6848. Brinck, T.; Murray, J. S.; Politzer, P. *J. Org. Chem.* **1991**, *56*, 5012−5015.
(12) Tsirelson, V. G.; Ozerov, R. P. *Electron Density and Bonding in Crystals*; Inst. of Physics Publ.: Bristol and Philadelphia, 1996.
(13) Roux, M.; Besnainou, S.; Daudel, R. *J. Chem. Phys.* **1956**, *53*, 218−223.
(14) Bader, R. F. W. In *Atoms in Molecules: A Quantum Theory*; The International Series of Monographs of Chemistry; Halpen, J., Green, M. L. H., Eds.; Clarendon Press: Oxford, 1990; pp 1−438.
(15) Bader, R. F. W. *Chem. Rev.* **1991**, *91*, 893−928.
(16) Tsirelson, V. G. *Can. J. Chem.* **1996**, *74*, 1171−1179.
(17) Bader, R. F. W.; Essen, H. *J. Chem. Phys.* **1984**, *80*, 1943−1960.
(18) Tsirelson, V. G.; Ivanov, Yu.; Zhurova, E. A.; Zhurov, V. V.; Tanaka, K. *Acta Crystallogr.* **2000**, *B56*, 197−203.
(19) Bader, R. F. W. *Phys. Rev.* **1994**, *B49*, 13348−13356.
(20) Matta, C. F.; Bader, R. F. W. *Proteins: Struct., Funct., Genet.* **2000**, *40*, 310−329.
(21) Pinkerton, A. A.; Schwarzenbach, D. ACA National Meeting, Hamilton, Ontario, Canada, Abstract PA22, June 22−27, 1986.
(22) Blessing, R. H. *Cryst. Rev.* **1987**, *1*, 3−58.
(23) DeTitta, G. T. *J. Appl. Crystallogr.* **1985**, *18*, 75−79.
(24) Sheldrick, G. M. SHELXTL Ver. 5.1. An Integrated System for Solving, Refining and Displaying Crystal Structures from Diffraction Data; University of Göttingen: Germany, 1997.
(25) Hansen, N.; Coppens, P. *Acta Crystallogr.* **1974**, *A34*, 909−921.

Table 1. Crystal Data and Structure Refinements

	(BIGH)(DN)	$(BIGH_2)(DN)_2$
empirical formula	$C_2H_8O_4N_8$	$C_2H_9O_8N_{11}$
temperature	90(1) K	90(1) K
crystal size	0.21 × 0.15 × 0.13 mm	0.32 × 0.23 × 0.13 mm
wavelength	0.71073 Å	0.71073 Å
crystal system	triclinic	monoclinic
space group	$P\bar{1}$	$C2/c$
unit cell dimensions	a = 4.280(1) Å, b = 9.288(1) Å, c = 10.530(4) Å, α = 85.34(2)°, β = 117.41(1)°, γ = 81.32(1)°	a = 11.667(2) Å, b = 8.131(1) Å, c = 12.973(1) Å, β = 117.41(1)°
unit cell θ range	$8 < \theta < 17°$	$11 < \theta < 29°$
V, Z	409.1 Å^3, 2	1096.8 Å^3, 4
$\omega/2\theta$ scan width	0.8 + 0.34 tan θ, °	1.0 + 0.34 tan θ, °
D(calc)	1.69 g cm^{-3}	1.91 g cm^{-3}
absorption coefficient	0.1443 mm^{-1}	0.1725 mm^{-1}
θ range	2.22−72.78°, $(\sin\theta/\lambda)_{max}$ = 1.34 Å^{-1}	3.17−73.04°, $(\sin\theta/\lambda)_{max}$ = 1.34 Å^{-1}
reflections collected	16 752	21 625
independent reflections	8275 (R_{int} = 0.0152)	9455 (R_{int} = 0.0238)
reflections used ($I > 4\sigma(I)$)	6095	5967
refinement method	full-matrix least-squares on F	full-matrix least-squares on F
weighting scheme	$1/\sigma^2(F_{obs})$	$1/\sigma^2(F_{obs})$
number of parameters	470	356
GOF	1.14	1.18
final R indices		
spherical atom refinement	0.0392	0.0390
aspherical atom refinement	0.0247	0.0201

multipole model as implemented in the XD program[26] was then used in further refinements. The positional and displacement parameters for the non-hydrogen atoms were refined with the high-angle reflections ($\sin\theta/\lambda > 0.7$ Å^{-1}). The multipole P_v, P_{lm}, κ, κ'-parameters and extinction were refined with the low-angle reflections ($\sin\theta/\lambda < 1.0$ Å^{-1}). For hydrogen atoms, all of the parameters including positional and displacement ones were refined with $\sin\theta/\lambda < 0.5$ Å^{-1}. The N−H bond lengths were then extended and fixed to the tabulated neutron values.[27] The scale factor refinement was carried out with all reflections, and the procedure was repeated until total convergence of the refined parameters. For the heavy atoms, the multipole refinement was performed up to the octapole level (l_{max} = 3) because all of the hexadecapole (l_{max} = 4) parameters appeared to be statistically insignificant. For the hydrogens, only dipole and quadrupole (l_{max} = 2) populations were refined. The molecule electroneutrality condition was imposed during the refinement. A total of seven κ-sets were used in the refinement with one value for all of the oxygens, one for all of the hydrogens, one for all of the carbons, but several values for the chemically distinct nitrogen atoms. For the $(BIGH_2)(DN)_2$ crystal, isotropic secondary extinction type I with a Gaussian mosaic distribution was described according to Becker and Coppens.[28] The y_{min} values were 0.48, 0.72, 0.73, and 0.77 for the (−4 0 4), (−1 1 3), (−1 1 4), and (−3 1 3) reflections, correspondingly. No extinction could be refined for the (BIGH)(DN) crystal. The rigid-bond test[29] showed that the differences of mean-square displacement amplitudes along the interatomic vectors were less than 1×10^{-4} Å^2 for the (BIGH)(DN) and 5×10^{-4} Å^2 for the $(BIGH_2)(DN)_2$ crystal. The largest least-squares correlation coefficients observed were 0.39 and 0.51. The statistical correctness of the weighting scheme (Table 1) and the final results were checked by the Abrahams and Keve test.[30] The atomic displacement ellipsoids (50% probability) are shown in Figure 1, the packing diagrams showing the hydrogen bonding schemes are in Figure 2, and the interatomic distances, the refined multipole, kappa, positional, and thermal parameters have been deposited. To estimate atomic spherical charges, a so-called κ-refinement[31] has been performed, the results of which have also been deposited.

Results and Discussion

(a) Electron Density Distributions. The residual electron density (the difference between experimental and calculated multipole EDs: $\delta\rho_{resid} = \rho_{exper} - \rho_{mult}$) maps were calculated with the low-angle reflections ($\sin\theta/\lambda < 1.0$ Å^{-1}). The largest residual is a minimum of −0.2 e Å^{-3} at the N(1) position in (BIGH)(DN); however, there are no peaks greater than ±0.1 e Å^{-3} on the interatomic bonds. For most of the bonds, the residual peaks do not exceed ±0.05 e Å^{-3}. These $\delta\rho_{resid}$ of ca. ±0.05 e Å^{-3} can be considered as the error estimations of the deformation ED. The maps have been deposited.

The dynamic multipole deformation EDs obtained from Fourier summations (the difference between calculated multipole and spherical EDs: $\delta\rho_{mult} = \rho_{mult} - \rho_{sph}$) are shown in Figures 3−5. Every expected covalent bond is represented by well-defined $\delta\rho_{mult}$ peaks. Electron lone pairs of oxygen, N(1), and N(6) [in (BIGH)(DN)] are also seen. Note that the oxygen lone pairs are located almost perpendicular to the N−O bonds and almost in the plane of the nitro groups (Figure 3). Similar disposition of the oxygen lone pairs has been observed in other neutral nitro compounds.[32−34] For the $(BIGH_2)(DN)_2$ crystal, the O(1) and O(2) lone pairs are slighly twisted out of the N(1)−N(2)−N(3) plane. The N(1) lone pairs in both crystals are significantly extended in the directions perpendicular to the N(1)−N(2)−N(3) plane (Figure 4). In the (BIGH)(DN) crystal, although the N(1)−N(3) bond (1.38 Å) is longer than the N(1)−N(2) bond (1.36 Å), the $\delta\rho_{mult}$ peaks have practically the same heights (0.35 and 0.34 e Å^{-3}, respectively). In $(BIGH_2)(DN)_2$, the difference in the N−N bond lengths is greater (1.35 and 1.39 Å), and the N(1)−N(3) $\delta\rho_{mult}$ peak is a little higher (0.34

(26) Koritsanszky, T.; Howard, S.; Mallison, P. R.; Su, Z.; Ritcher, T.; Hansen, N. K. XD. A Computer Program Package for Multipole Refinement and Analysis of Electron Densities from Diffraction Data. User's Manual; University of Berlin: Germany, 1995.
(27) Allen, F. H.; Kennard, O.; Watson, D. G.; Brammer, L.; Orpen, A. G.; Taylor, R. *J. Chem. Soc., Perkin Trans. 2* **1987**, S1−S19.
(28) Becker, P. J.; Coppens, P. *Acta Crystallogr.* **1974**, *A30*, 129−147.
(29) Hirshfeld, F. L. *Acta Crystallogr.* **1976**, *A32*, 239−244.
(30) Abrahams, S. C.; Keve, E. T. *Acta Crystallogr.* **1971**, *A27*, 157−165.
(31) Coppens, P.; Guru Row, T. N.; Leung, P.; Stevens, E. D.; Becker, P. J.; Yang, Y. W. *Acta Crystallogr.* **1979**, *A35*, 63−72.
(32) Chen, Yu-Sh.; Pinkerton, A. A. **2001**, to be published.
(33) Zhurova, E. A.; Pinkerton, A. A. *Acta Crystallogr.* **2001**, *B57*, 359−365.
(34) Kubicki, M.; Borowiak, T.; Ditkiewicz, G.; Souhassou, M.; Jelsch, C.; Lecomte, C. *J. Phys. Chem.* **2002**, *106*, 3706−3714.

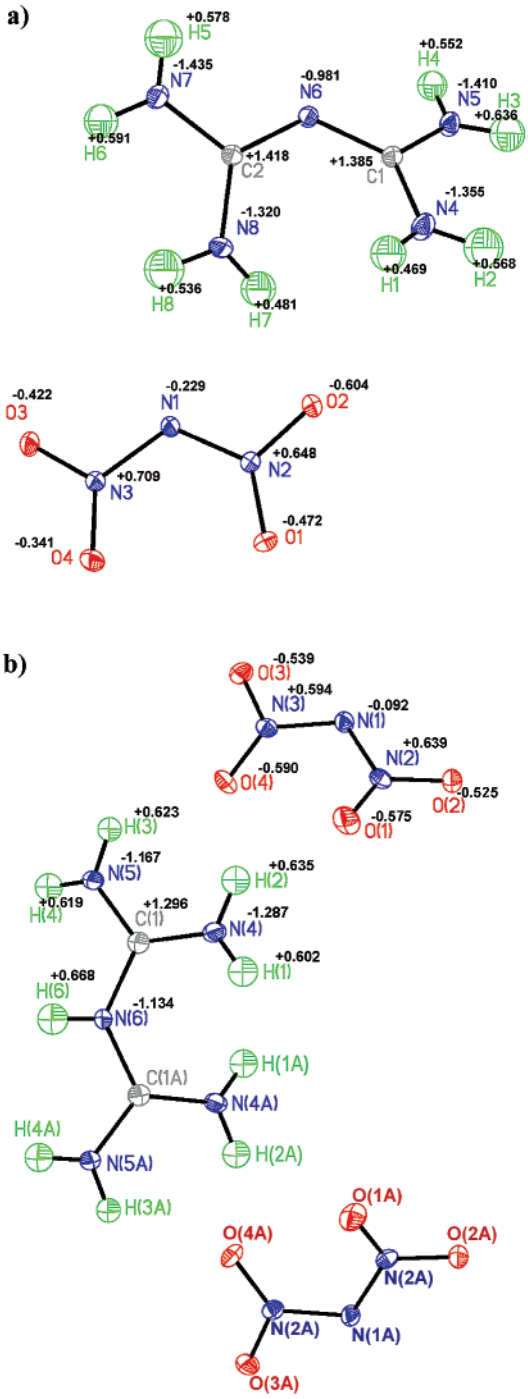

Figure 1. The (BIGH)(DN) (a) and $(BIGH_2)(DN)_2$ (b) molecules with 50% atomic displacement ellipsoids overlaid with atomic charges integrated over atomic basins (see text for details). In $(BIGH_2)(DN)_2$, the N(6)−H(6) bond coincides with the 2-fold crystallographic axis. The total charge of the (DN) anion is −0.711 e^- for (BIGH)(DN) and −1.087 e^- for $(BIGH_2)(DN)_2$.

as compared with 0.30 e $Å^{-3}$), but this difference is not significant with respect to the errors (±0.05 e $Å^{-3}$). In $(BIGH_2)(DN)_2$, the N−N $\delta\rho_{mult}$ is observed to be more diffuse in agreement with the N(2),N(3) κ'-parameter being 0.838(8) in (BIGH)(DN) and 0.827(5) in $(BIGH_2)(DN)_2$. The N(6) (cation) lone pair in (BIGH)(DN) (Figure 4c) is more compact than those of N(1) (anions), having it's maximum slightly shifted away from the N(6)−C(1)−C(2) plane toward an associated H(4) atom. The N(6)−C bonds are more diffuse in the dication in $(BIGH_2)(DN)_2$ as compared to the monocation in (BIGH)(DN)

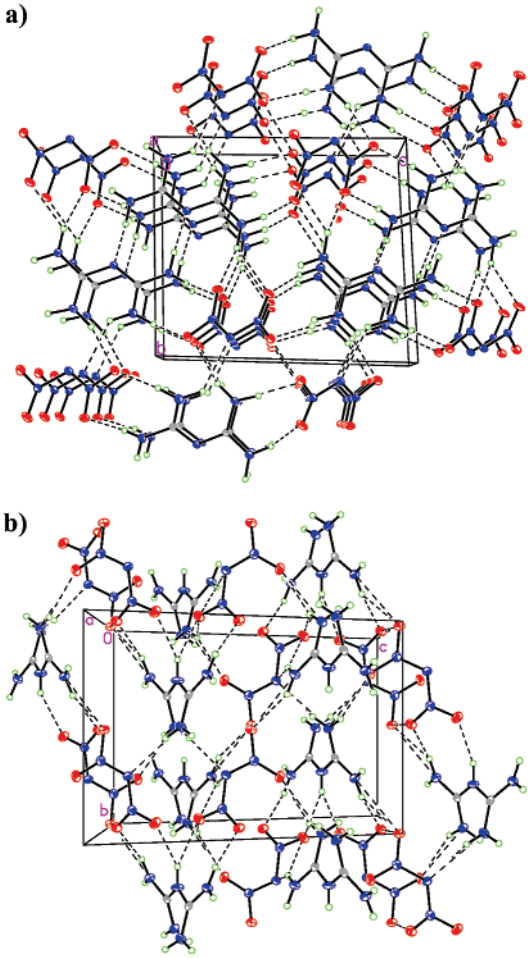

Figure 2. The packing diagrams of (BIGH)(DN) (a) and $(BIGH_2)(DN)_2$ (b). The oxygen, nitrogen, carbon, and hydrogen atoms are represented by red, blue, gray, and green ellipsoids, correspondingly.

(Figure 5) [N(6) κ' is 0.90(2) for (BIGH)(DN) and 0.84(2) for $(BIGH_2)(DN)_2$]. In the $(BIGH_2)(DN)_2$ crystal, the N(6) and H(6) atoms are located on the 2-fold axis, so the N(6)−C(1) and N(6)−C(1A) bonds are exactly equal. The N(6)−C(1) and N(6)−C(2) bond lengths are almost equal in (BIGH)(DN) being 1.34 Å, but the $\delta\rho_{mult}$ peak on the N(6)−C(1) bond of 0.46 e $Å^{-3}$ is a little greater than that on the N(6)−C(2) bond of 0.38 e $Å^{-3}$. Although this difference is still within the estimated maximum ED error of 0.1 e $Å^{-3}$, it will be shown below that the topological analysis of the total ED gives us a more satisfactory picture of the chemical bonds in these crystals. The C(1)−N(4) and C(1)−N(5) [and C(2)−N(7), C(2)−N(8)] bond lengths differ by 0.1 Å in (BIGH)(DN), the shorter bonds having greater $\delta\rho_{mult}$ peaks (by ∼0.1 e $Å^{-3}$), as expected.

(b) Topological Analysis of the Electron Density. The topological analysis was performed with the XD[26] and TOPXD[35] programs. Using the static multipole model of the ED, we found the (3,−1) critical points characterizing the covalent and hydrogen bonding in the crystals (Tables 2 and 3). For every atom, all of the interactions within a 5 Å cluster were taken into account. The second lines in Tables 2 and 3 contain the data for the procrystal constructed from overlapping neutral spherical atoms. It is clear, that for every expected covalent

(35) Volkov, A.; Gatti, C.; Abramov, Yu.; Coppens, P. *Acta Crystallogr.* **2000**, *A56*, 252−258.

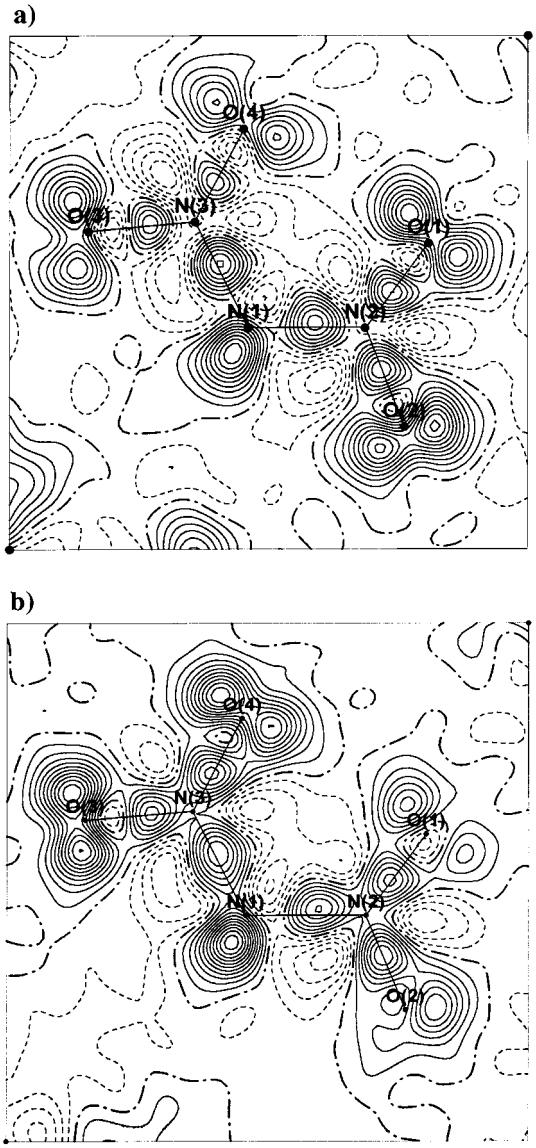

Figure 3. The multipole deformation electron density ($\delta\rho_{mult} = \rho_{mult} - \rho_{sph}$) maps of the (DN) anion of (BIGH)(DN) (a) and $(BIGH_2)(DN)_2$ (b) in the N(1)−N(2)−N(3) plane. The contour interval is 0.05 e Å^{-3}.

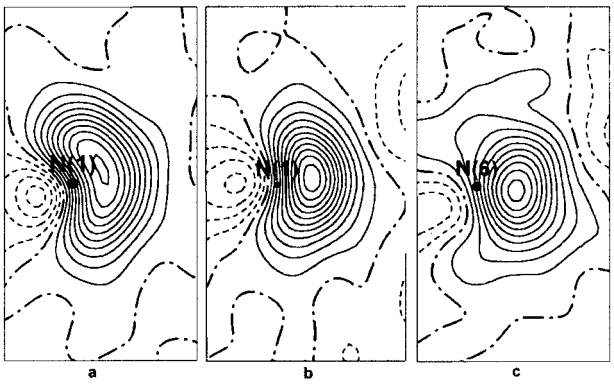

Figure 4. The N(1) electron lone pair of (BIGH)(DN) (a) and $(BIGH_2)$-$(DN)_2$ (b) in the plane perpendicular to N(1)−N(2)−N(3); the N(6) lone pair of (BIGH)(DN) (c). The contour interval is 0.05 e Å^{-3}.

bond, there is a significant contraction of the ED toward the CP in the directions perpendicular to the interatomic lines (λ_1 and λ_2) as compared to the neutral procrystal. Together with smaller values of λ_3 curvatures, this results in the negative

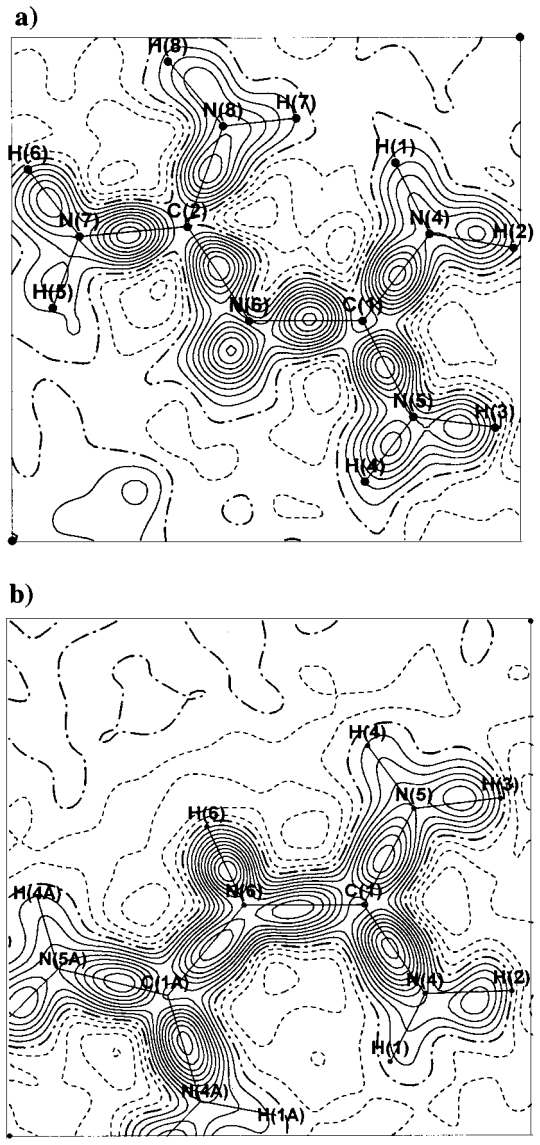

Figure 5. The multipole deformation electron density ($\delta\rho_{mult} = \rho_{mult} - \rho_{sph}$) maps of (BIGH)(DN) (a) and $(BIGH_2)(DN)_2$ (b) in the N(6)−C(1)−C(2)/C(1A) plane. The contour interval is 0.05 e Å^{-3}. All of the hydrogen atoms are twisted out of this plane.

Laplacian values at the CPs showing the shared character of the atomic interactions.[14]

Analysis of the chemical bonds indicates significant conjugation of all the bonds in the dinitramide anion, as well as the N−C bonds in the cations. The highest ED values are observed for the N−O bonds, whereas the smallest ED values are observed for the single N−H bonds. The ellipticities of the conjugated bonds are generally higher than those for the N−H bonds. For the (DN) anion, the properties at the CPs can be compared with the theoretical values calculated for the isolated dinitramide anion at the B3LYP/6-311+G(d) level.[8] The experimental ED values at the CPs agree within 4% with those from the theoretical calculations,[8] although the experimental Laplacian values are systematically more positive. This tendency in the Laplacian values has been observed before[33] and could be a result of limited flexibility of the N and O radial functions adopted in the multipole ED model.[36] For the N−N bonds in the (DN) anion, the expected correspondence between the bond lengths and ED values at the bond CPs is observed: the shorter

Table 2. Bond Critical Points in the (BIGH)(DN) Crystal[a]

bond path	ρ, e Å^{-3}	$\nabla^2\rho$, e Å^{-5}	λ_1, e Å^{-5}	λ_2, e Å^{-5}	λ_3, e Å^{-5}	R_{ij}, Å	d_1, Å	d_2, Å	D, kJ/mol	$\epsilon = \lambda_1/\lambda_2 - 1$
N(1)−N(2)	2.47(3)	−8.22(8)	−22.26	−16.99	31.02	1.359	0.645	0.714		0.31
	2.06	8.23	−13.18	−12.94	34.35	1.359	0.678	0.681		0.02
N(1)−N(3)	2.34(3)	−6.41(8)	−20.37	−15.99	29.96	1.381	0.648	0.733		0.27
	1.96	8.91	−12.41	−12.16	33.48	1.381	0.689	0.692		0.02
O(1)−N(2)	3.36(4)	−15.4(1)	−32.98	−27.54	45.12	1.231	0.631	0.600		0.20
	2.88	8.56	−21.21	−21.03	50.80	1.231	0.662	0.569		0.01
O(2)−N(2)	3.28(4)	−12.3(1)	−30.96	−26.79	45.41	1.248	0.635	0.613		0.16
	2.78	9.95	−20.32	−20.05	50.31	1.248	0.667	0.581		0.01
O(3)−N(3)	3.22(4)	−10.9(1)	−30.90	−25.06	45.02	1.235	0.631	0.604		0.23
	2.86	9.01	−20.98	−20.72	50.70	1.235	0.663	0.572		0.01
O(4)−N(3)	3.24(4)	−11.1(1)	−31.36	−24.77	45.00	1.226	0.627	0.599		0.27
	2.91	8.12	−21.50	−21.31	50.93	1.226	0.660	0.566		0.01
N(6)−C(1)	2.38(4)	−22.0(1)	−20.12	−16.54	14.63	1.344	0.756	0.588		0.22
	1.78	−3.37	−9.15	−8.88	14.66	1.344	0.776	0.568		0.03
N(6)−C(2)	2.33(4)	−20.9(1)	−19.85	−15.43	14.38	1.340	0.755	0.585		0.29
	1.79	−3.58	−9.20	−8.93	14.55	1.340	0.775	0.565		0.03
N(4)−C(1)	2.38(3)	−29.3(2)	−21.47	−16.47	9.07	1.341	0.816	0.525		0.27
	1.79	−3.55	−9.18	−8.89	14.53	1.341	0.777	0.564		0.03
N(5)−C(1)	2.52(4)	−29.6(2)	−22.24	−18.66	11.29	1.334	0.771	0.563		0.19
	1.81	−3.91	−9.28	−8.94	14.31	1.334	0.776	0.558		0.04
N(7)−C(2)	2.44(3)	−31.0(2)	−21.58	−17.97	8.52	1.337	0.819	0.518		0.20
	1.80	−3.73	−9.25	−8.91	14.43	1.337	0.776	0.561		0.04
N(8)−C(2)	2.34(3)	−26.9(2)	−20.84	−15.48	9.44	1.334	0.812	0.522		0.35
	1.81	−3.93	−9.26	−8.97	14.30	1.334	0.776	0.558		0.03
N(4)−H(1)	2.04(3)	−23.0(2)	−26.93	−24.01	27.95	1.009	0.765	0.244		0.12
	1.57	−8.70	−17.21	−17.12	25.64	1.009	0.763	0.246		0.01
N(4)−H(2)	2.11(4)	−32.2(2)	−30.12	−26.97	24.93	1.009	0.774	0.235		0.12
	1.57	−8.70	−17.24	−17.11	25.65	1.009	0.763	0.246		0.01
N(5)−H(3)	2.07(4)	−32.7(2)	−29.75	−26.46	23.47	1.009	0.778	0.231		0.12
	1.57	−8.71	−17.24	−17.12	25.65	1.009	0.763	0.246		0.01
N(5)−H(4)	2.02(4)	−27.9(2)	−29.43	−24.97	26.51	1.009	0.785	0.224		0.18
	1.57	−8.69	−17.23	−17.12	25.66	1.009	0.763	0.246		0.01
N(7)−H(5)	2.16(4)	−34.1(2)	−31.06	−29.41	26.34	1.009	0.792	0.217		0.06
	1.57	−8.72	−17.23	−17.13	25.65	1.009	0.763	0.246		0.01
N(7)−H(6)	2.12(4)	−33.8(2)	−30.14	−29.40	25.74	1.009	0.787	0.222		0.03
	1.57	−8.72	−17.24	−17.12	25.64	1.009	0.763	0.246		0.01
N(8)−H(7)	2.09(3)	−27.8(2)	−28.86	−27.17	28.23	1.009	0.781	0.228		0.06
	1.57	−8.69	−17.21	−17.12	25.64	1.009	0.763	0.246		0.01
N(8)−H(8)	2.09(4)	−28.4(2)	−28.76	−25.33	25.69	1.009	0.765	0.244		0.14
	1.57	−8.70	−17.24	−17.12	25.65	1.009	0.763	0.246		0.01
O(3)···H(8),	0.13(3)	2.53(4)	−0.91	−0.58	4.02	1.948	1.247	0.701	21.3	0.57
{$-x-y-z$, (001)}	0.21	2.27	−0.97	−0.95	4.19	1.942	1.167	0.775		0.02
O(2)···H(2),	0.13(3)	1.98(3)	−0.91	−0.66	3.54	1.985	1.264	0.719	19.3	0.39
{$-x-y-z$, (200)}	0.198	2.134	−0.88	−0.87	3.88	1.976	1.181	0.795		0.02
N(6)···H(4),	0.15(3)	2.42(4)	−1.06	−0.60	4.07	1.996	1.302	0.694	24.8	0.78
{$-x-y-z$, (110)}	0.21	1.96	−0.89	−0.85	3.70	1.995	1.205	0.790		0.05
O(2)···H(7)	0.15(1)	1.58(2)	−0.84	−0.63	3.04	2.078	1.268	0.810	20.6	0.33
	0.17	1.86	−0.68	−0.640	3.18	2.078	1.227	0.851		0.07
O(1)···H(5),	0.09(2)	1.82(2)	−0.50	−0.40	2.73	2.103	1.314	0.789	13.7	0.25
{xyz, (0−10)}	0.16	1.81	−0.68	−0.65	3.14	2.073	1.221	0.852		0.04
O(1)···H(3),	0.06(3)	1.53(3)	−0.43	−0.29	2.25	2.134	1.363	0.771	9.6	0.47
{$-x-y-z$, (200)}	0.17	1.88	−0.72	−0.69	3.29	2.052	1.215	0.837		0.04
O(4)···H(6),	0.07(2)	1.00(2)	−0.36	−0.31	1.67	2.278	1.432	0.846	7.9	0.17
{$-x-y-z$, (001)}	0.11	1.28	−0.40	−0.38	2.06	2.265	1.304	0.961		0.05
O(4)···H(5),	0.06(1)	1.43(1)	−0.29	−0.17	1.89	2.321	1.370	0.951	9.1	0.64
{xyz, (0−10)}	0.11	1.38	−0.42	−0.34	2.14	2.262	1.293	0.969		0.22
N(1)···H(1),	0.06(1)	0.990(8)	−0.254	−0.223	1.466	2.480	1.474	1.006	7.4	0.14
{xyz, (−100)}	0.09	0.970	−0.275	−0.256	1.501	2.435	1.395	1.140		0.08
O(3)···H(8),	0.03(1)	0.840(8)	−0.107	−0.081	1.028	2.782	1.272	1.510	4.5	0.32
{xyz, (−100)}	0.06	0.863	−0.191	−0.098	1.152	2.630	1.413	1.217		0.94
O(1)···O(4)	0.12(1)	2.40(1)	−0.50	−0.46	3.36	2.531	1.270	1.261		0.09

[a] We report the values of the electron density (ρ), Hessian eigenvalues (λ_1, λ_2, and λ_3) and Laplacian ($\nabla^2\rho = \lambda_1 + \lambda_2 + \lambda_3$) at the critical point, the distances from the critical point to the first and second atoms (d_1 and d_2), their sum ($R_{ij} = d_1 + d_2$), the ellipticity of the bond (ϵ), and the dissociation energy D estimated for hydrogen bonds. The first line contains the experimental results; the second line contains the data for the atomic procrystal.

bonds have significantly higher ED values at the CPs. For the N−C bonds in the cations, the shorter bonds also have higher ED values. The "equivalent" N(6)−C(1) and N(6)−C(2) bonds in (BIGH)(DN) have the same ED value at the CPs within 1.25 standard deviations. Significant polarization of all bonds is observed, as the CPs are shifted toward the less electronegative atoms. It is interesting that at the N(1)−N(2) and N(1)−N(3) bonds of the dinitramide anion, the CP position is shifted toward the N(1) atom. The same effect is observed in ammonium dinitramide crystals[37] and in a series of other energetic com-

(36) Bianchi, R.; Gatti, C.; Adovasio, V.; Nardelli, M. *Acta Crystallogr.* **1996**, *B52*, 471−478. Volkov, A.; Abramov, Yu.; Coppens, P.; Gatti, C. *Acta Crystallogr.* **2000**, *A56*, 332−339. Iversen, B. B.; Larsen, F. K.; Figgis, B. N.; Reynolds, P. A. *J. Chem. Soc., Dalton Trans.* **1997**, 2227−2240.

(37) Zhurova, E. A.; Martin, A.; Pinkerton, A. A. 2001, unpublished result.

Table 3. Bond Critical Points in $(BIGH_2)(DN)_2$[a]

bond path	ρ, e Å^{-3}	$\nabla^2\rho$, e Å^{-5}	λ_1, e Å^{-5}	λ_2, e Å^{-5}	λ_3, e Å^{-5}	R_{ij}, Å	d_1, Å	d_2, Å	D, kJ/mol	$\epsilon = \lambda_1/\lambda_2 - 1$
N(1)−N(2)	2.22(1)	−4.24(4)	−19.36	−15.41	30.53	1.391	0.662	0.729		0.25
	1.92	9.16	−12.09	−11.84	33.09	1.390	0.694	0.696		0.02
N(1)−N(3)	2.50(1)	−7.42(4)	−22.86	−17.81	33.26	1.354	0.654	0.700		0.28
	2.08	8.10	−13.33	−13.08	34.51	1.354	0.676	0.678		0.02
O(1)−N(2)	3.45(2)	−11.29(5)	−32.00	−28.60	49.31	1.220	0.625	0.595		0.12
	2.96	7.54	−21.86	−21.68	51.08	1.220	0.658	0.562		0.01
O(2)−N(2)	3.47(2)	−13.08(5)	−33.30	−29.56	49.77	1.230	0.639	0.591		0.12
	2.89	8.58	−21.26	−21.01	50.85	1.230	0.661	0.569		0.01
O(3)−N(3)	3.16(2)	−5.85(5)	−28.26	−25.32	47.73	1.248	0.634	0.614		0.11
	2.78	9.95	−20.31	−20.05	50.31	1.247	0.667	0.580		0.01
O(4)−N(3)	3.34(2)	−8.66(5)	−30.46	−27.25	49.05	1.229	0.629	0.600		0.12
	2.90	8.38	−21.33	−21.15	50.86	1.229	0.661	0.568		0.01
N(6)−C(1)	2.20(1)	−18.75(5)	−17.93	−15.90	15.08	1.370	0.793	0.577		0.13
	1.70	−1.71	−8.78	−8.48	15.56	1.369	0.780	0.589		0.04
N(4)−C(1)	2.61(2)	−28.15(6)	−23.24	−18.70	13.79	1.312	0.768	0.544		0.24
	1.87	−5.28	−9.53	−9.24	13.49	1.312	0.775	0.537		0.03
N(5)−C(1)	2.50(1)	−25.38(5)	−21.66	−17.97	14.26	1.319	0.765	0.554		0.20
	1.85	−4.82	−9.45	−9.13	13.77	1.319	0.775	0.544		0.04
N(4)−H(1)	2.12(2)	−33.2(1)	−33.24	−30.48	28.70	1.009	0.779	0.230		0.06
	1.57	−8.69	−17.22	−17.13	25.66	1.009	0.763	0.246		0.01
N(4)−H(2)	2.06(2)	−31.6(1)	−29.10	−26.92	24.45	1.009	0.772	0.237		0.08
	1.57	−8.73	−17.25	−17.13	25.65	1.009	0.764	0.245		0.01
N(5)−H(3)	2.00(2)	−30.6(1)	−28.80	−27.38	25.54	1.009	0.787	0.222		0.05
	1.57	−8.72	−17.24	−17.13	25.65	1.009	0.763	0.246		0.01
N(5)−H(4)	2.10(2)	−33.6(1)	−30.60	−28.92	25.91	1.009	0.785	0.224		0.06
	1.57	−8.71	−17.24	−17.13	25.65	1.009	0.763	0.246		0.01
N(6)−H(6)	1.97(2)	−34.7(1)	−32.59	−28.47	26.33	1.009	0.811	0.198		0.15
	1.57	−8.69	−17.26	−17.08	25.65	1.010	0.764	0.245		0.01
N(1)···H(1),	0.15(1)	2.33(2)	−1.04	−0.81	4.18	1.955	1.304	0.651	23.8	0.27
{0.5 + *x*, 0.5 − *y*,	0.23	2.08	−0.98	−0.96	4.02	1.954	1.183	0.771		0.03
0.5 + *z*, (−1 1 −1)}										
O(4)···H(4),	0.11(1)	1.63(1)	−0.61	−0.57	2.81	2.073	1.325	0.748	14.8	0.07
{0.5 − *x*, 0.5 − *y*, −*z*}	0.16	1.84	−0.68	−0.66	3.18	2.069	1.219	0.850		0.02
O(1)···H(2)	0.063(8)	1.728(9)	−0.351	−0.280	2.359	2.174	1.333	0.841	11.0	0.27
	0.150	1.719	−0.607	−0.587	2.913	2.113	1.234	0.879		0.04
O(3)···H(6),	0.095(3)	1.263(3)	−0.533	−0.340	2.136	2.220	1.380	0.840	11.9	0.85
{0.5 − *x*, 0.5 − *y*, −*z*}	0.134	1.572	−0.493	−0.469	2.533	2.181	1.265	0.916		0.05
O(3)···H(3),	0.062(9)	1.150(8)	−0.291	−0.271	1.712	2.286	1.444	0.842	8.3	0.15
{−*x*, −*y*, −*z*, (010)}	0.112	1.338	−0.396	−0.239	1.972	2.290	1.325	0.965		0.66
O(2)···H(4),	0.044(6)	1.347(4)	−0.235	−0.163	1.745	2.412	1.394	1.018	7.8	0.41
{*x*, *y*, *z*, (010)}	0.107	1.331	−0.383	−0.301	2.015	2.305	1.305	1.000		0.27
O(3)···H(2),	0.032(5)	0.756(3)	−0.153	−0.122	1.030	2.630	1.578	1.052	4.4	0.41
{−*x*, −*y*, −*z*, (010)}	0.074	0.934	−0.236	−0.198	1.368	2.465	1.379	1.086		0.19
O(4)···H(3)	0.035(3)	0.677(1)	−0.149	−0.110	0.937	2.776	1.490	1.286	4.2	0.31
	0.055	0.738	−0.149	−0.121	1.008	2.642	1.438	1.204		0.24
O(1)···O(4)	0.12(1)	2.35(1)	−0.43	−0.40	3.19	2.562	1.283	1.279		0.08

[a] The definition of the values is the same as in Table 2.

pounds[32,33] as well. As a result of this polarization, the effective N(1) negative charge, integrated over the atomic volume (see below), is less than it would be in a nonpolarized case. Critical points between the closest oxygens in the (DN) anion in both compounds have been located as well. The analysis of this interaction has been reported elsewhere.[38]

The Laplacian maps for the dinitramide anions are shown in Figure 6, and other Laplacian maps have been deposited. The solid contours show the negative values of the Laplacian; that is, they represent the accumulation of ED in the crystal. This accumulation is mostly concentrated around the atoms along the chemical bonds and in the nonbonding directions associated with lone pairs. No elongation of the N(1) Laplacian peaks in the nonbonding direction (both in the N(1)−N(2)−N(3) and in the perpendicular plane) is observed in contrast to the features seen in the deformation electron density maps (Figures 6 and 7b). All of the Laplacian peaks are compact and well shaped. The $-\nabla^2\rho(\mathbf{r})$ peaks not associated with chemical bonds can be considered as the preferred sites of protonation with oxygen atoms having higher $-\nabla^2\rho(\mathbf{r})$ peaks as compared to those of nitrogens.

(c) Hydrogen Bonding. Significant hydrogen bonding can be expected in these crystals, and only those interactions with interatomic distances less than 3 Å are shown in Tables 2 and 3. Details of the hydrogen bonding scheme have been discussed earlier.[3] It is worth noting that most of the H atoms are involved in two hydrogen bonds with different oxygen atoms and vice versa. In the (BIGH)(DN) crystal, the O(3) atom associates with two H(8) atoms at the same time, the nearest one at a distance of 1.948 Å, and one from a symmetry related molecule at 2.782 Å. The values of $\rho(\mathbf{r}_c)$ at the hydrogen bond CPs are a little higher than those with similar bond lengths previously reported (see, for example, Espinosa et al.,[39] Coppens et al.[40]). However, it is important to keep in mind that, in this case, the hydrogen bonding is accompanied by electrostatic cation−anion interactions. The ED values at the CPs are lower when compared to the procrystals, thus stressing the closed-shell type of these interactions.

(38) Zhurova, E. A.; Tsirelson, V. G.; Stash, A. I.; Pinkerton, A. A. *J. Am. Chem. Soc.* **2002**, *124*, 4574−4575.

(39) Espinosa, E.; Souhassou, M.; Lachekar, H.; Lecomte, C. *Acta Crystallogr.* **1999**, *B55*, 563−572.

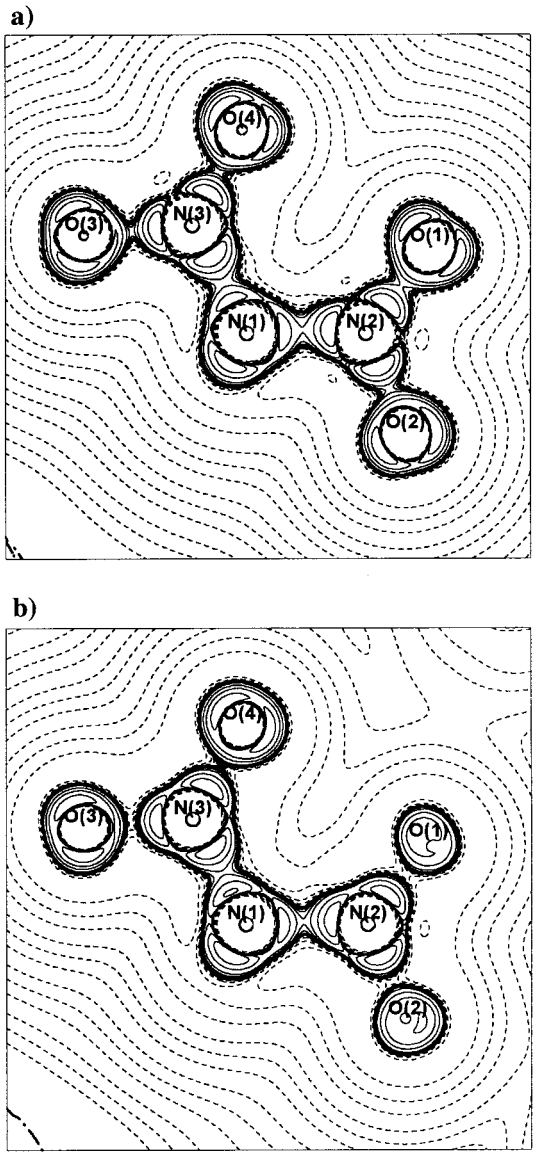

Figure 6. The negative Laplacian of the electron density of (BIGH)(DN) (a) and $(BIGH_2)(DN)_2$ (b) in the N(1)−N(2)−N(3) plane. The contour interval is 2,4,8 × 10^{-3-+3} e $Å^{-5}$.

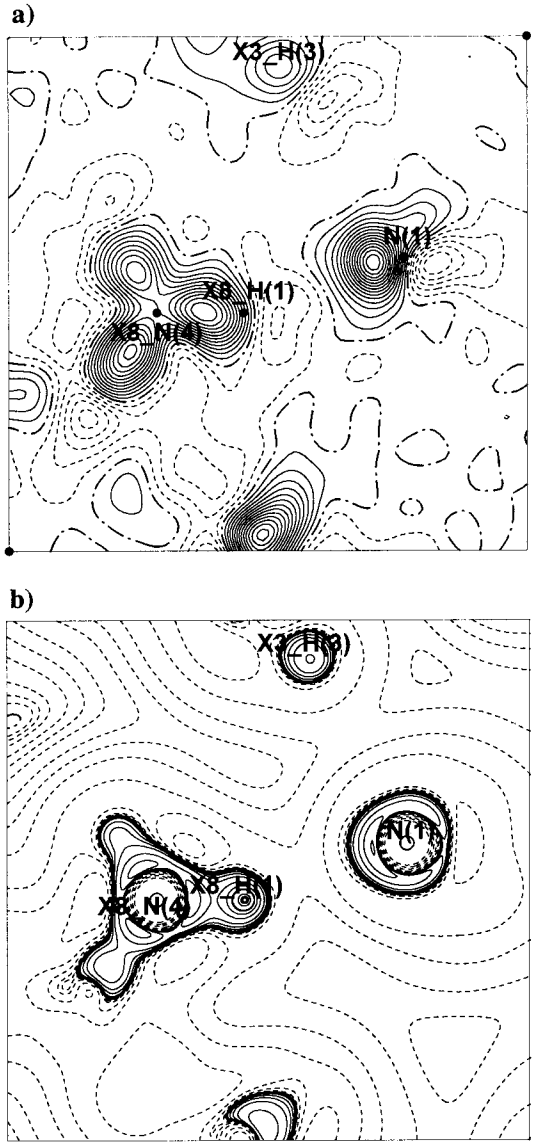

Figure 7. The multipole deformation electron density (a) and the negative Laplacian of the electron density (b) in the N(1)···H(1) hydrogen bond region in the $(BIGH_2)(DN)_2$ crystal. X8_N(4) and X8_H(1) are the atoms N(4) and H(1) obtained using symmetry operator {0.5 + *x*, 0.5 − *y*, 0.5 + *z*, (−1 1 −1)}; X3_H(3) is the H(3) atom obtained using operator {−*x*, −*y*, −*z*, (0 1 0)}. The N(4)−H(1)−N(1) plane is shown; contours are as in Figures 3 and 6 plus a contour of 70 e $Å^{-5}$ for Figure 7b.

Following Espinosa et al.,[41] the dissociation energies for the hydrogen bonds have been estimated as

$$D = -v(\mathbf{r}_c)/2$$

Here $v(\mathbf{r}_c)$ is a potential energy density at the CP, which in turn can be calculated from the local form of the virial theorem:[14]

$$2g(\mathbf{r}_c) + v(\mathbf{r}_c) = (1/4)\nabla^2\rho(\mathbf{r}_c)$$

The kinetic energy at the CP $g(\mathbf{r}_c)$ can be calculated[42] from the values of the ED $\rho(\mathbf{r}_c)$ and the Laplacian $\nabla^2\rho(\mathbf{r}_c)$ at the CP from Kirzhnits gradient expansion[43] of the one-particle Green function around the Thomas−Fermi term. At the CP:

$$g(\mathbf{r}_c) = (3/10)(3\pi^2)^{2/3}\rho(\mathbf{r}_c)^{5/3} + 1/6\nabla^2\rho(\mathbf{r}_c)$$

These dissociation energies are shown in the 10th columns of Tables 2 and 3. Although for the $(BIGH_2)(DN)_2$ crystal, the shortest hydrogen bond has the highest dissociation energy, this is not the case for the (BIGH)(DN) crystal. The shortest is the O(3)···H(8) bond, whereas the strongest hydrogen bond is created by the N(6) atom of the cation in agreement with the strong exothermic second protonation energy.[7] We consider the ellipticities of these bonds to be meaningless because of the small values of λ_1, λ_2.

(40) Coppens, P.; Abramov, Yu.; Carducci, M.; Korjov, B.; Novozhilova, I.; Alhambra, C.; Pressprich, M. *J. Am. Chem. Soc.* **1999**, *121*, 2585−2593.
(41) Espinosa, E.; Molins, E.; Lecomte, C. *Chem. Phys. Lett.* **1998**, *285*, 170−173.
(42) Masunov, A. E.; Vyboishchikov, S. F. XVI Intern. Crystallogr. Congress. Collected Abstracts: Beijing, 1993; p 380. Abramov, Yu. A. *Acta Crystallogr.* **1997**, *A53*, 264−272. Tsirelson, V. G. *Acta Crystallogr.* **2002**, *B58*, in press.
(43) Kirzhnits, D. A. *Sov. Phys. JETP* **1957**, *5*, 64−71.

Table 4. The Atomic Basin Volumes, Å^3

	(BIGH)(DN)	$(BIGH_2)(DN)_2$
O(1)	14.76	15.15
O(2)	15.67	14.39
O(3)	14.51	15.42
O(4)	17.09	14.55
N(1)	12.86	12.52
N(2)	6.02	6.27
N(3)	6.28	6.36
N(4)	16.85	15.33
N(5)	17.91	15.66
N(6)	14.75	14.49
N(7)/N(5A)	20.29	15.66
N(8)/N(4A)	15.98	15.33
C(1)	5.27	4.92
C(2)/C(1A)	5.67	4.92
H(1)	2.88	1.81
H(2)	2.38	1.89
H(3)	2.09	2.14
H(4)	2.37	1.94
H(5)/H(4A)	2.19	1.94
H(6)		1.69
H(6)/H(3A)	3.07	2.14
H(7)/H(1A)	2.53	1.81
H(8)/H(2A)	2.44	1.89
molecular volume	203.9	272.9
molecular volume × Z [a]	407.8	1091.5
unit cell volume	409.1	1096.8

[a] Z is the number of molecules in a unit cell.

The deformation ED and the Laplacian maps for the shortest N(1)···H(1) hydrogen bond in $(BIGH_2)(DN)_2$ are shown in Figure 7. The polarization of the N(1) electron density can be clearly seen. On the N(4)−H(1) line, the deformation ED peak is shifted from H(1) toward the N(4) atom, as is expected for a H atom involved in hydrogen bonding.[44] However, this polarization is not as high as is observed for very strong hydrogen bonds.[33,45] Although the N(1) peaks of the $\delta\rho_{mult}(\mathbf{r})$ and $\nabla^2\rho(\mathbf{r})$ functions are directed toward the H(1) atom, their maxima are slightly shifted from the N(1)···H(1) line toward the H(3) atom. Nevertheless, no critical point was found between the N(1) and H(3) atoms (2.36 Å), and, according to Bader,[46] no bonding interaction exists between these two atoms.

(d) Atomic Charges and Volumes. The atomic basin boundaries were defined, and some of the atomic properties were integrated within the basins with the TOPXD program.[35] The integrated atomic charge $q(\Omega)$ over the atomic basin Ω is defined as a difference between nuclear Z_Ω and electronic $N(\Omega)$ charges:

$$q(\Omega) = Z_\Omega - N(\Omega)$$

$$N(\Omega) = \int_\Omega \rho(\mathbf{r})\mathrm{d}\tau$$

where $\rho(\mathbf{r})$ is the electron density.

The atomic charges thus derived are shown in Figure 1. The electroneutrality condition was fulfilled up to 0.002 e^- for the (BIGH)(DN) and 0.0004 e^- for the $(BIGH_2)(DN)_2$ crystals. The atomic basin volumes are reported in Table 4. As expected, they are generally larger for the negative atoms and much smaller for the positive atoms. The good agreement between the molecular volume, multiplied by the number of molecules in the unit cell and the unit cell volume, demonstrates the quality of the atomic partitioning of space. The atomic charges, calculated from AIM theory, are generally higher[35] than those one would expect from the spherical atom model[31] (see deposited material) or Mulliken analysis. Nevertheless, the AIM analysis, being based on first principles, gives a more rigorous definition of the atomic charges. Every charge, shown in Figure 1, has a reasonable value and sign expected for this type of compound. These charges can be compared with those calculated using AIM theory applied for the theoretical data for the (DN) anion:[8] $q_{O(1),O(2),O(3),O(4)} = -0.51\,e^-$, $q_{N(1)} = -0.18\,e^-$, $q_{N(2),N(3)} = +0.63\,e^-$. These values are very close to the average of our experimental charges (−0.51, −0.16, and +0.65 e^-, respectively). It will be particularly interesting to compare these atomic charges and volumes with those from nonexplosive compounds when more AIM studies of the nitro-compounds will be available. Currently, the only data available for nonenergetic materials are for *p*-nitroaniline[35] and 1-phenyl-4-nitroimidazole,[34] for molecular energetic materials for NTO,[47] and for ionic energetic materials for the current compounds. The values are reported in Table 5. Although there is an apparent enhancement of nitrogen charge and reduction in the atomic volumes for energetic materials, it is premature to draw conclusions from such a small sample of compounds.

Table 5. AIM Atomic Charges (e Å^{-3})/Volumes (Å^3) of the Nitro Group Nitrogen Atoms in Various Organic Compounds

compound	O	N
p-nitroaniline	−0.45/17.2[a]	+0.18/7.9
1-phenyl-4-nitro-imidazole	−0.35, −0.48/17.59, 17.03	+0.21/8.16
NTO	−0.38, −0.35/16.33, 15.22	+0.50/6.70
(BIGH)(DN)	−0.47, −0.60, −0.42, −0.34/14.76, 15.67, 14.51, 17.09	+0.65, +0.71/6.02, 6.28
$(BIGH_2)(DN)_2$	−0.58, −0.53, −0.54, −0.59/15.15, 14.39, 15.42, 14.55	+0.64, +0.59/6.27, 6.36

[a] Average values.

Conclusion

We have obtained the multipole model parameters for the electron density distribution in biguanidinium dinitramide and biguanidinium bis-dinitramide from experimental X-ray diffraction data and analyzed some of the physical and chemical properties of these compounds using Bader's topological theory. For these molecules, the topological theory provides a more satisfactory description of the chemical bonding as compared to the classical analysis of the deformation densities. The significantly shorter N−N bond of the dinitramide anion has a higher value of the electron density and a more negative Laplacian at the bond critical point, although the deformation electron density peaks are of almost the same height. The geometry of oxygen's lone pairs was found far from the expected sp^2 configuration; the lone pairs are located approximately perpendicular to the N−O bonds and almost in the plane of the nitro groups. The N(1) lone pairs are significantly extended perpendicular to the N(1)−N(2)−N(3) plane. Signifi-

(44) Krijn, M. P. C. M.; Graafsma, H.; Feil, D. *Acta Crystallogr.* **1988**, *B44*, 609−616.
(45) Zavodnik, V.; Stash, A.; Tsirelson, V.; De Vries, R.; Feil, D. *Acta Crystallogr.* **1999**, *B55*, 45−54.
(46) Bader, R. W. F. *J. Phys. Chem.* **1998**, *A102*, 7314−7323.
(47) Zhurova, E. A.; Tsirelson, V. G.; Stash, A. I.; Yakovlev, M.; Pinkerton, A. A. *J. Phys. Chem.* **2002**, submitted.

cant conjugation of all the bonds in the dinitramide anion, as well as N−C bonds in the cations, was found. The atomic charges and volumes have been determined by the integration over the atomic basins. The extensive hydrogen bonding was analyzed, and the dissociation energies were estimated for hydrogen bonds.

Acknowledgment. We appreciate the financial support of the Office of Naval Research through contract number N00014-95-1-0013. We thank Dr. A. Volkov and Prof. P. Coppens for making the TOPXD program available for us and for valuable comments.

Supporting Information Available: Tables of refined parameters, distances and angles, and maps of the residual, deformation and Laplacian of the electron density, and the electrostatic potential (PDF). This material is available free of charge via the Internet at http://pubs.acs.org.

JA0176245